



# Microbeam analysis techniques for the characterisation of irradiated nuclear fuel

Stéphane Brémier

European Commission, Joint Research Centre,

Institute for Transuranium Elements

Karlsruhe, Germany



to contribute to European efforts in the **nuclear fuel and fuel cycle research**



- to increase the useful life and safety of nuclear fuel in commercial power stations
- to improve the spent fuel behavior under intermediate and final storage conditions
- to reduce the amount and the toxicity of radioactive waste (P&T)

#### Hot Cell facilities at ITU

- 24 hot cells (licensed capacity  $10^6$  Ci =  $3.7 \cdot 10^{16}$  Bq)
- ~ 160 kg of irradiated fuel (80 LWR fuel rods) and 3.5 kg Pu
- shielded SEM, OM, EPMA, SIMS, XRD
- infrastructure: supporting workshop incl. manipulators maintenance
- 3 hot labs for characterization of non-irradiated materials

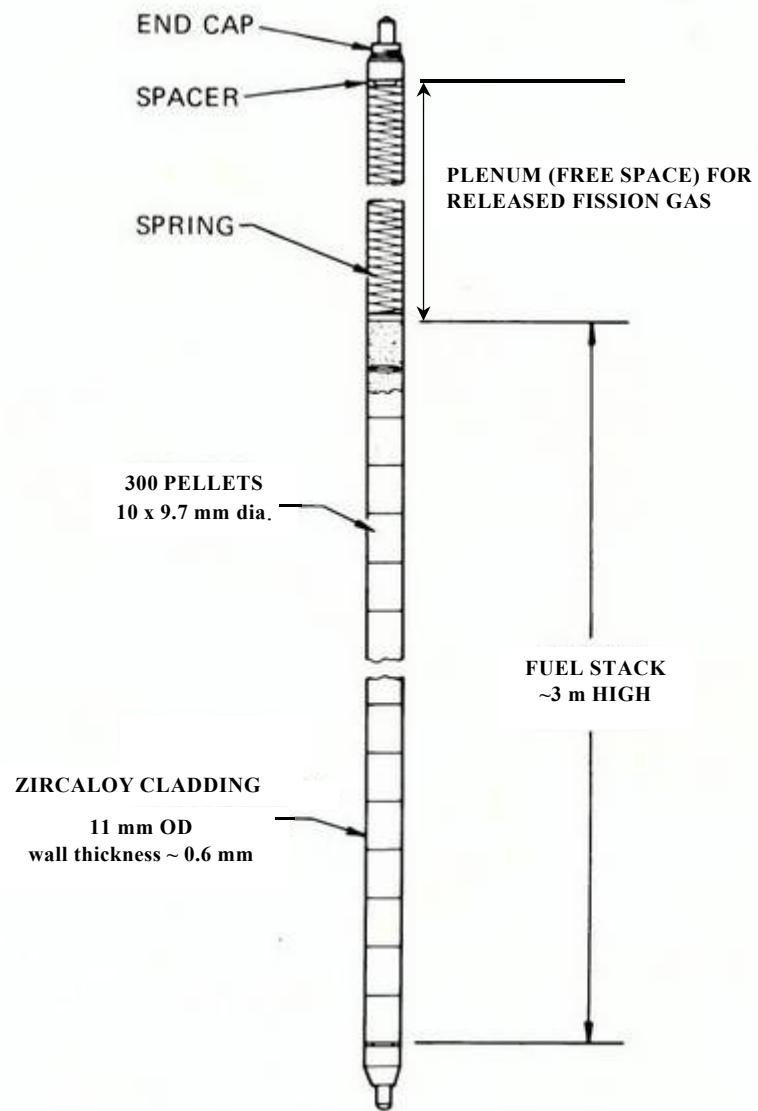
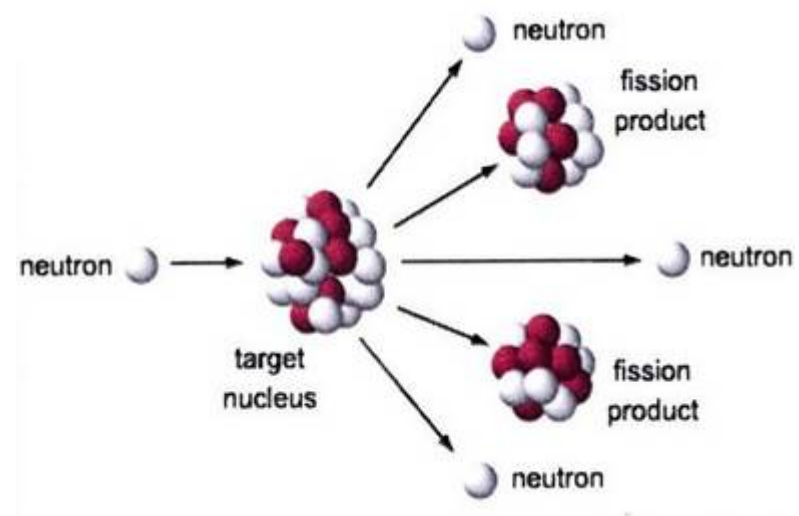


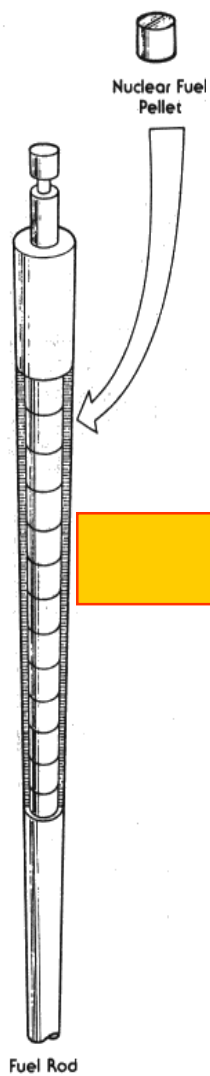
## Diagram of a PWR Rod

The fuel rod is filled with helium up to a pressure of 25 bar. The gas provides a path for heat conduction across the gap between the fuel pellets and the Zircaloy cladding.





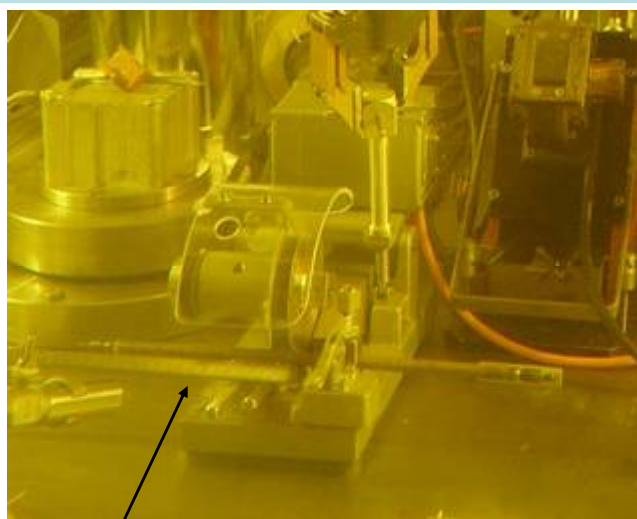
European  
Commission



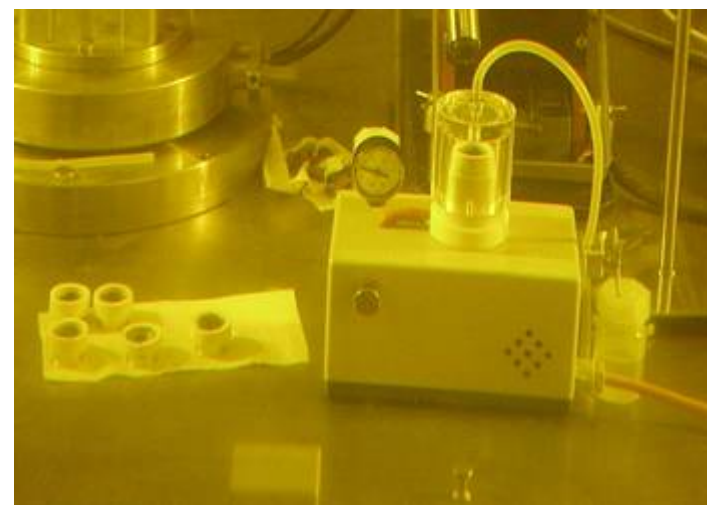
Irradiated fuel rods are transported in shielded containers



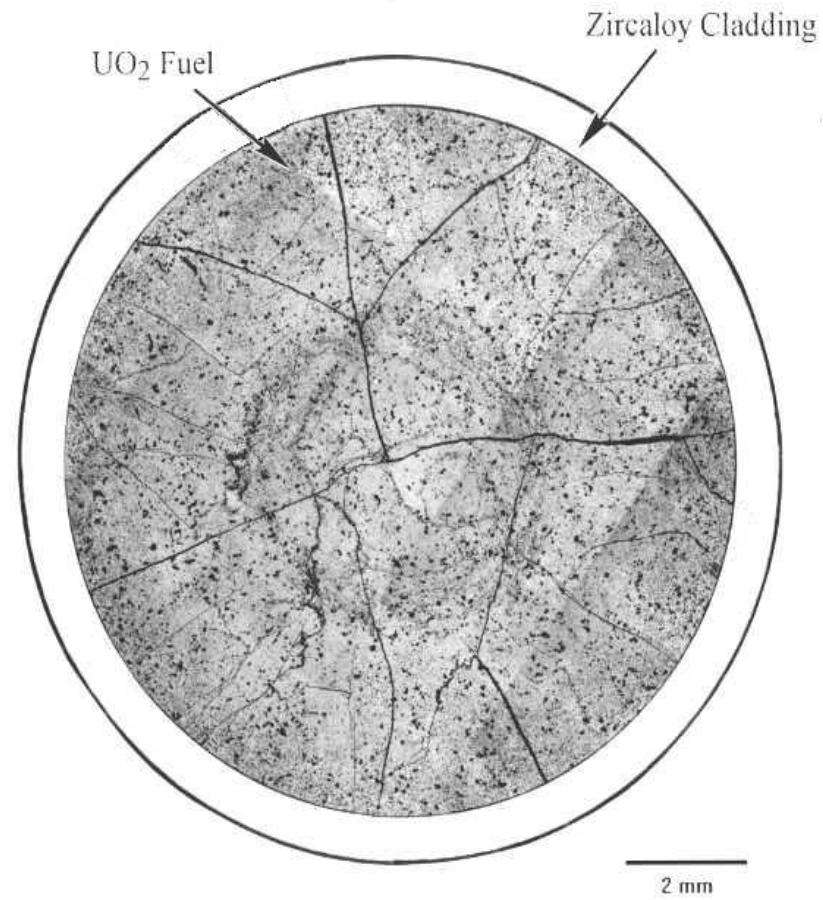
Unloading the content in the hot cell B1



Fuel pin inside cutting machine



Embedding of cut samples



A sample of UO<sub>2</sub> nuclear fuel prepared for EPMA.



## Sample Preparation for microbeam analysis techniques

Four main steps:

1. Standard metallographic preparation in an hot cell.
2. Decontamination.
3. Mounting of the specimen in the capsule together with the reference materials needed for EPMA.
4. Transport of the specimen to the shielded microprobe or sims using a lead cask.

## Cameca SX100R shielded Microprobe



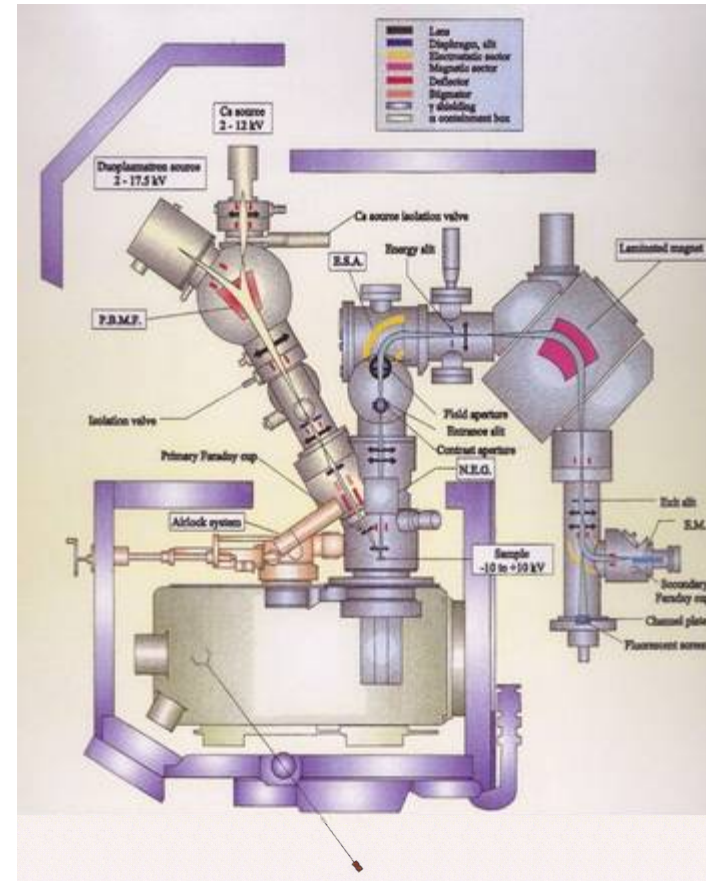
Views of the Cameca SX100R electron microprobe for the analysis of irradiated nuclear fuel at the Institute for Transuranium Elements.



## Cameca IMS 6FR shielded Secondary Ion Mass Spectrometer



Front view of the installation showing the lead cell and glove box.



General diagram of the shielded IMS 6FR Secondary Ion Mass Spectrometer (Courtesy of CAMECA, France).

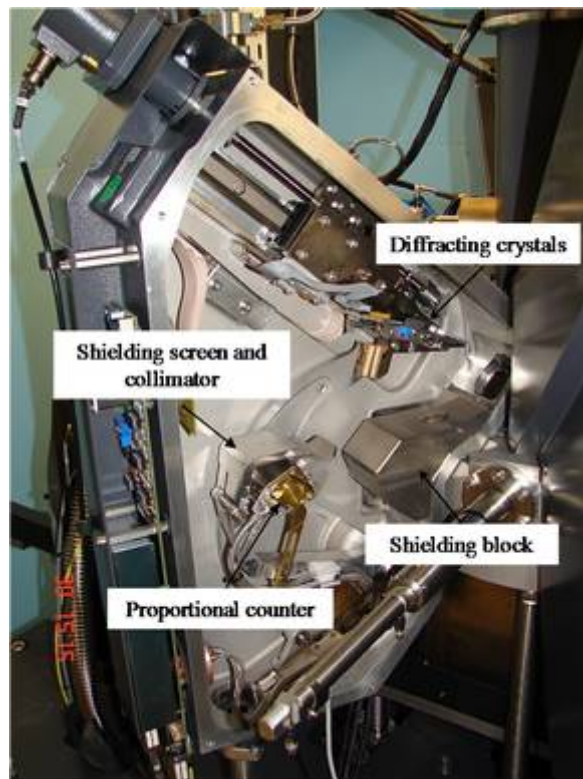


## EPMA of Nuclear Fuel

### Differences from Standard EPMA

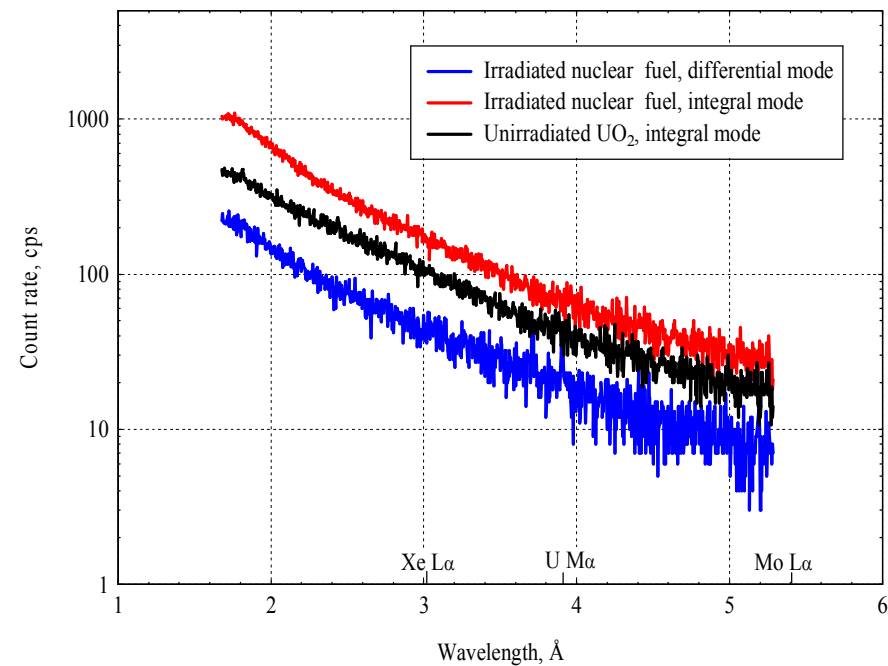
- The microprobe operator must be protected from radiation exposure.
- For the actinide elements, U, Np, Pu, Am and Cm, the M X-ray lines are used.
- For quantitative fission product analysis, trace element techniques are employed.

## SX100 R spectrometer



View inside one of the spectrometers of the Cameca shielded SX100R electron microprobe. A tungsten block is placed where the spectrometer joins the specimen chamber and the proportional counter is located behind an INERMET screen.

## PHA settings

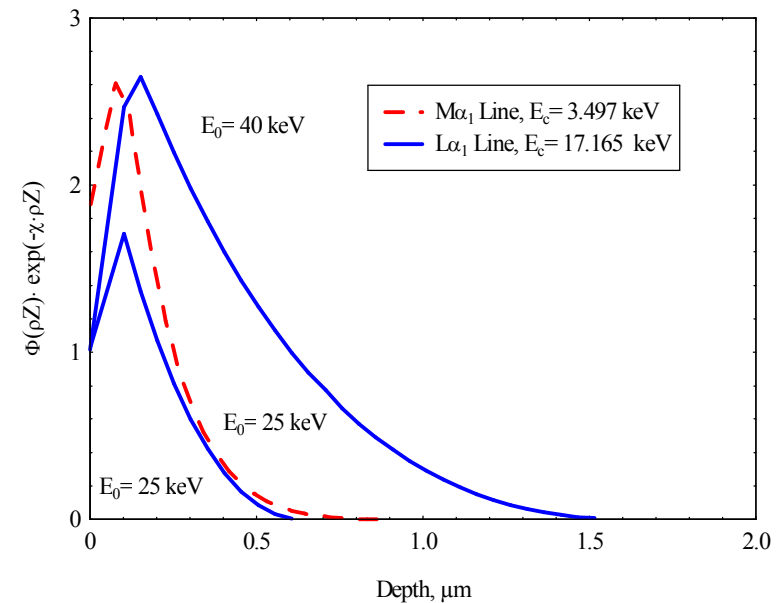


Effect of shielding and pulse height discrimination on the irradiation background when working with a 1011 quartz crystal (used for the analysis of uranium and plutonium). The  $\gamma$  dose rate from the irradiated fuel sample at 30 cm distance was of the order of  $1.5 \text{ mSv h}^{-1}$ .

## Critical excitation potential and lowest recommended electron accelerating voltage for the L- and M-lines of the actinide elements

Element	Critical Excitation Potential, keV		Potential, keV		$E_0^a$ , kV	
	$L\alpha_1$	$L\beta_1$	$M\alpha_1$	$M\beta$	$L\alpha_1$	$M\alpha_1$
Th	16.30	19.68	3.33	3.49	41	8
U	17.17	20.95	3.55	3.73	43	9
Np	17.62	21.6	3.67	3.85	44	9
Pu	18.07	22.27	3.78	3.97	45	9
Am	18.50	22.94	3.89	4.09	46	10
Cm	18.93	23.78	3.97	4.23	47	10

a. 2.5x the critical excitation potential.



At an electron acceleration potential of 25 keV about 20% more X-ray intensity is obtained using the  $M\alpha$  line without significant increase in the X-ray excitation depth.



European Commission

# Analysis Conditions used for the Actinide Elements at the Institute for Transuranium Elements

Element	X-ray line	Diffracting Crystal	$E_0$ (kV)	Beam Current (nA)	Standards
Th	$M\alpha_1$	Quartz (1011)	20 or 25*	100 or 250*	$ThO_2$
U	$M\alpha_1$	Quartz (1011)	20 or 25*	100 or 250*	$UO_2$
Np	$M\alpha_1$	Quartz (1011)	20 or 25*	100 or 250*	$NpO_2$
Pu	$M\beta$	Quartz (1011)	20 or 25*	100 or 250*	$PuO_2$
Am	$M\beta$	Quartz (1011)	20 or 25*	100 or 250*	$PuO_2$
Cm	$M\beta$	Quartz (1011)	20 or 25*	100 or 250*	$PuO_2$

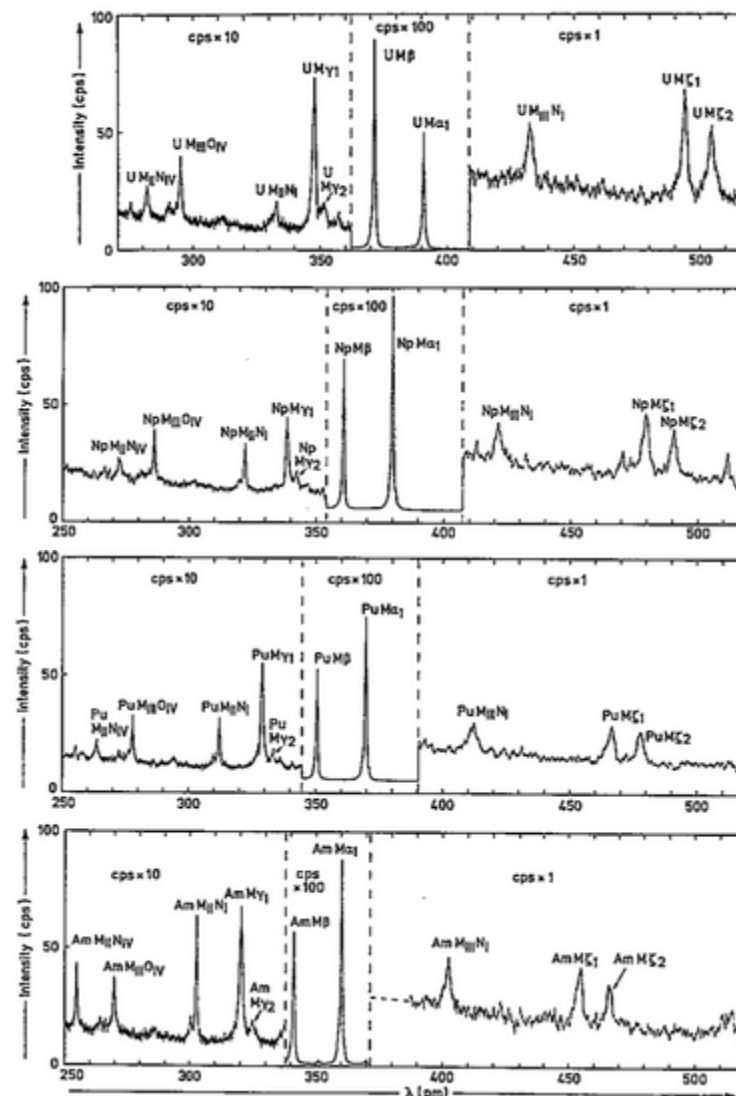
\* when fission gas analysed simultaneously

Performance Indicator	Quartz 1011	PET
Sensitivity ( $c \cdot s^{-1} \cdot \mu A^{-1}$ )	$8.4 \times 10^4$	$1.9 \times 10^5$
P/B ratio	97	105
line width <sup>a</sup> , $\Delta\lambda/\lambda$ (Å)	0.0024	0.0032
Overlap with U $M\beta$ line <sup>b</sup> (%)	8.2	9.4

Camaca SX 100. Beam voltage 20 kV

a. FWHM

b. Intensity of the U  $M\beta$  line at the peak position of the Pu  $M\alpha_1$  as a percentage of the intensity of the latter.

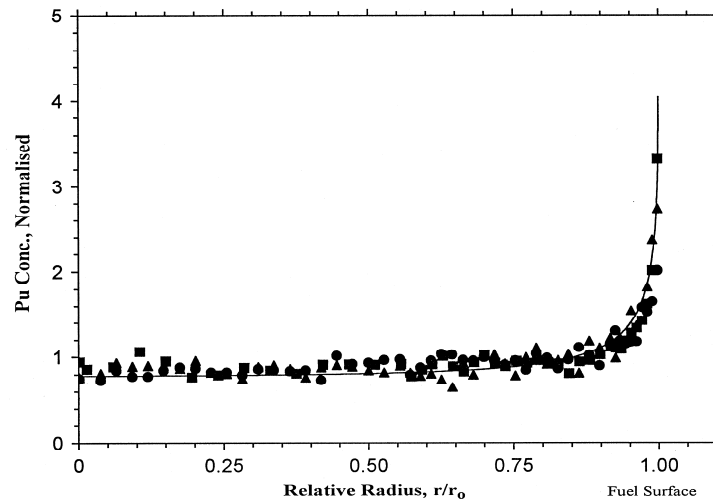




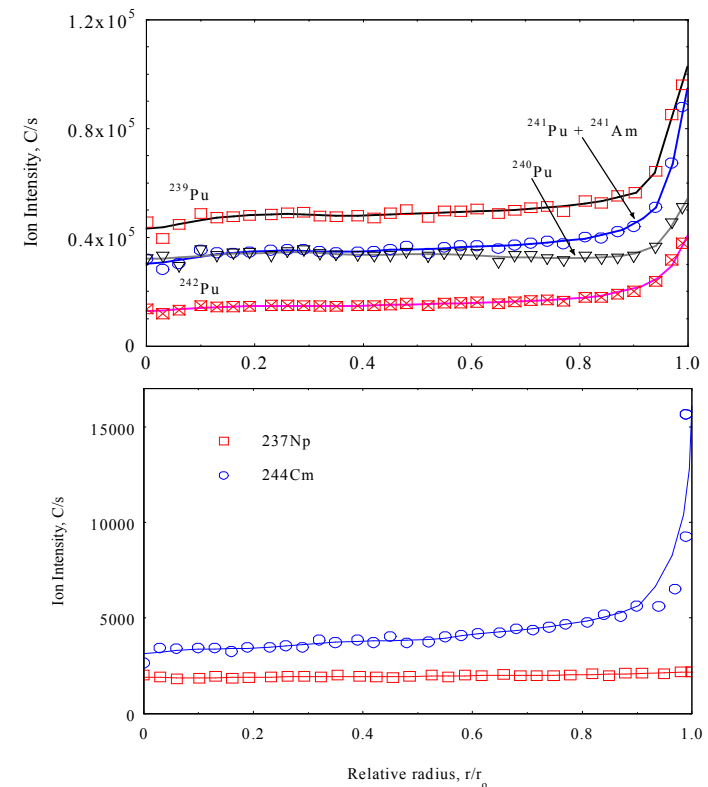
## Microbeam analysis techniques employed in the investigation of irradiated nuclear fuel rods

Technique	Applications
WDS-EMPA	Radial burn-up distribution Plutonium concentration Fission Product Behaviour Fission gas release Characterisation of Corium Characterisation of the microstructure of MOX fuel Evolution of the high burn-up structure
SEM	Characterisation of the high burn-up structure Zirconium hydride formation in Zircaloy cladding
SIMS	Gas pressure in bubbles in nuclear fuel Behaviour of minor fission products and minor actinides Behaviour of the fission gas krypton Radial variation in the stoichiometry of irradiated $UO_2$ fuel Role Li and B in water-side corrosion of Zircaloy
TEM	characterisation intragranular gas bubbles
REM	characterisation of intra- and intergranular gas bubbles
micro-XRF	Fission gas release
micro-XRD	Oxidation state Irradiation damage High burn-up structure Local solubility of fission products

## Determination of the radial distribution of the actinides in a UO<sub>2</sub> fuel matrix

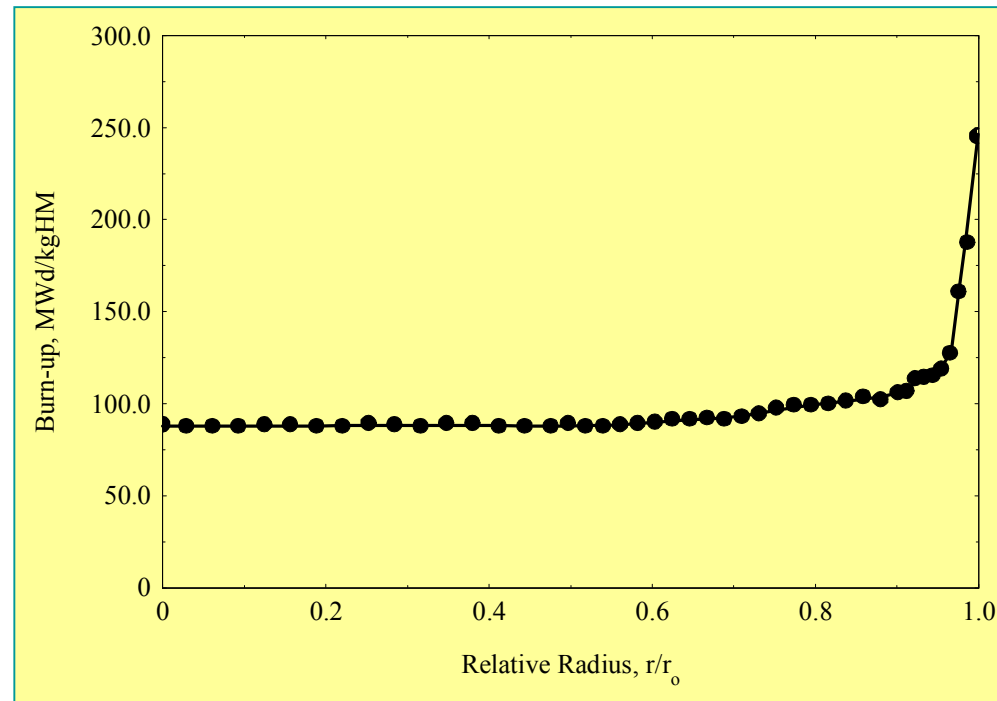


EPMA point analysis results for the radial distribution of Pu in 30 MWd/kgHM UO<sub>2</sub> fuels



- Pu, Am, Cm isotopes produced by capture of epithermal neutrons by <sup>238</sup>U
- <sup>237</sup>Np originate from capture of thermal neutrons by <sup>235</sup>U

## Measurement of the local burn-up in irradiated nuclear fuel



**The radial burn-up distribution in a  $\text{UO}_2$  nuclear fuel pellet with an average burn-up of about 100 MWd/kgHM. The local burn-up increases sharply at the fuel surface due to the fission of plutonium created from uranium by neutron capture.**



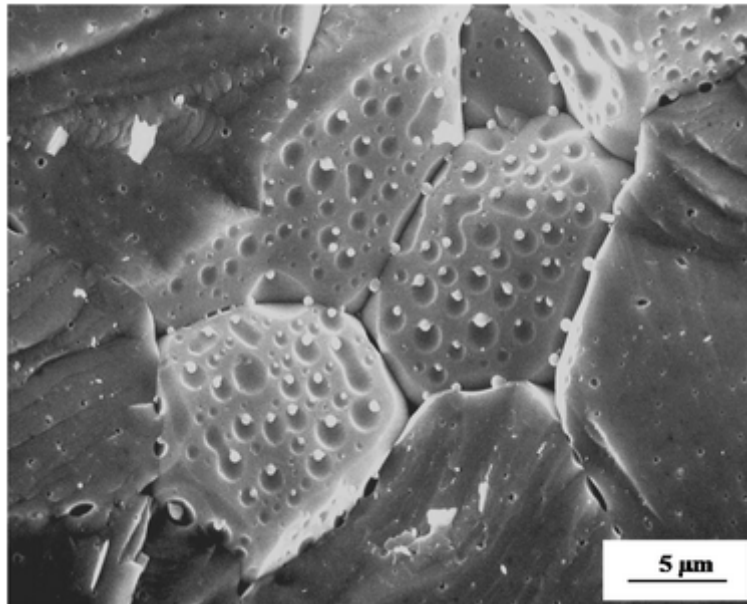
## Fission Gas Behaviour

The inert gases **Xe and Kr** constitute around **30%** of the fission products produced during irradiation.

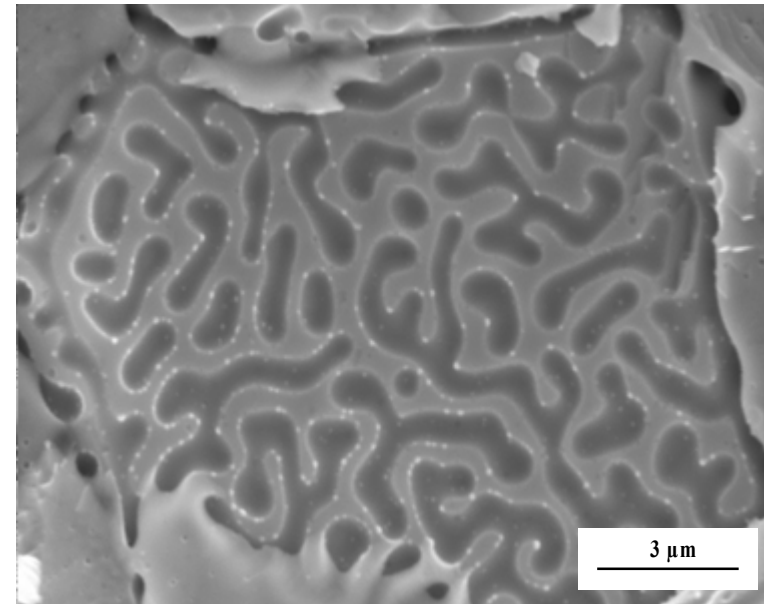
1. Consequences of the high temperature in the central part of the fuel pellet
2. Consequences of the increasing burn-up in the outer part of the fuel pellet

## Effect of temperature 1/3

At temperatures below about  $1000^{\circ}\text{C}$  the gas atoms are dispersed in the fuel matrix; above  $1000^{\circ}\text{C}$  part of the gas atoms coalesce to form bubbles and part are released to the rod free volume.



Microstructures of  $\text{UO}_2$  nuclear fuel that has experienced a temperature above  $1000^{\circ}\text{C}$ . Gas bubbles are present on the grain faces and within the grains.

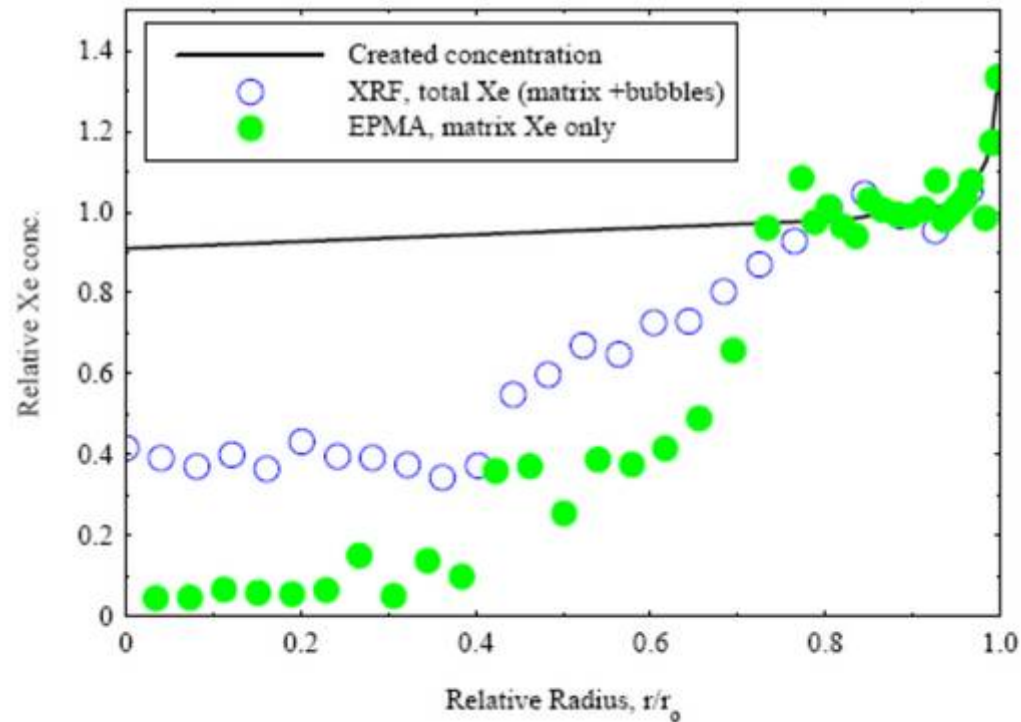


SEM micrograph of vermicular gas pores on a grain face in a  $\text{UO}_2$  nuclear fuel formed by the interconnection of individual spherical bubbles.

## Consequences of Gas Bubble Formation in Nuclear Fuel

- **The formation of gas bubbles causes the fuel to expand, or swell. At high burn-up swelling can result in increased mechanical interaction between the fuel and its containment which can eventually lead to rod failure.**
- **The presence of gas bubbles decreases the thermal conductivity of the fuel (similar effect to porosity) which leads to an increase in the fuel operating temperature.**

## Distribution of the Fission Gas Xe

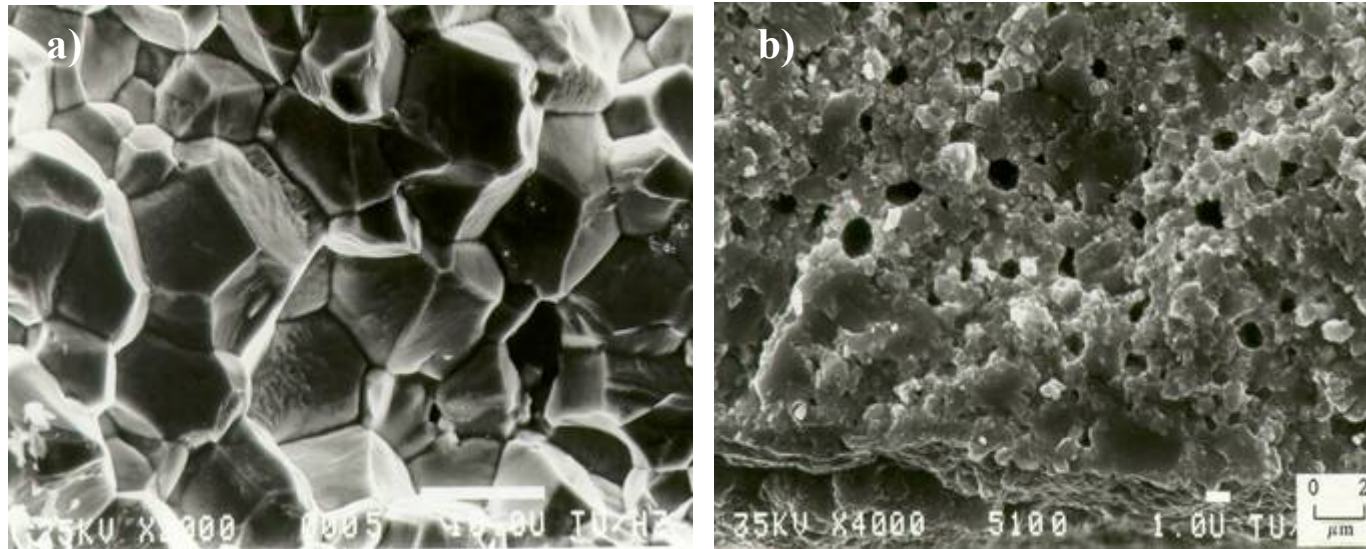


The radial distribution of xenon retained in a  $\text{UO}_2$  fuel subjected to reactor power excursion to  $40 \text{ Wm}^{-1}$  at a burn-up of  $50 \text{ MWd/kgHM}$  as revealed by EPMA and XRF. The difference between the two profiles corresponds to the amount of gas in bubbles.

## The High Burn-up Structure

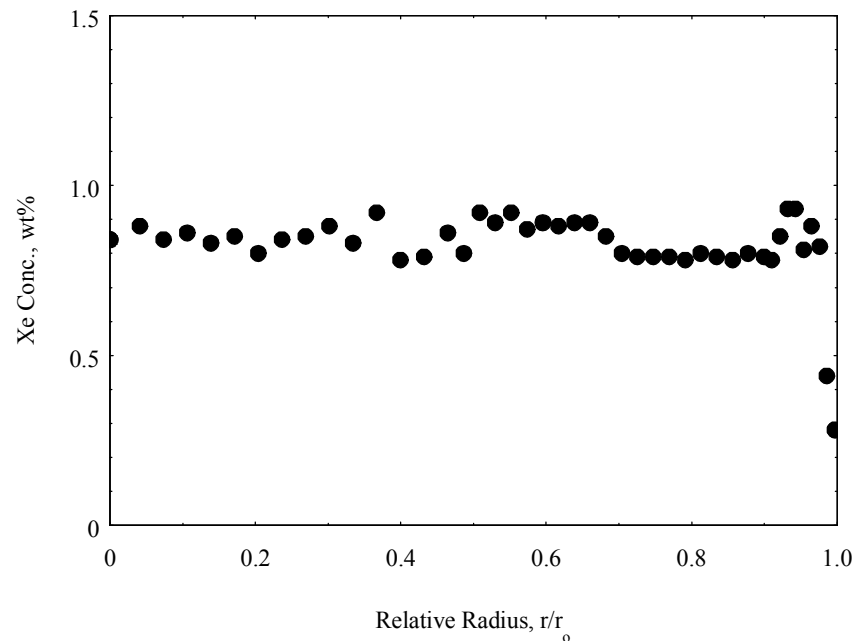
### Characteristics:

- **Pronounced decrease in grain size from 10  $\mu\text{m}$  to typically 0.15  $\mu\text{m}$ .**
- **High concentration of small gas pores of typical diameter 1 to 2  $\mu\text{m}$ .**
- **Considerable loss of fission gas from the fuel matrix. The concentration of xenon falls from about 1 wt% to 0.2 to 0.3 wt%.**

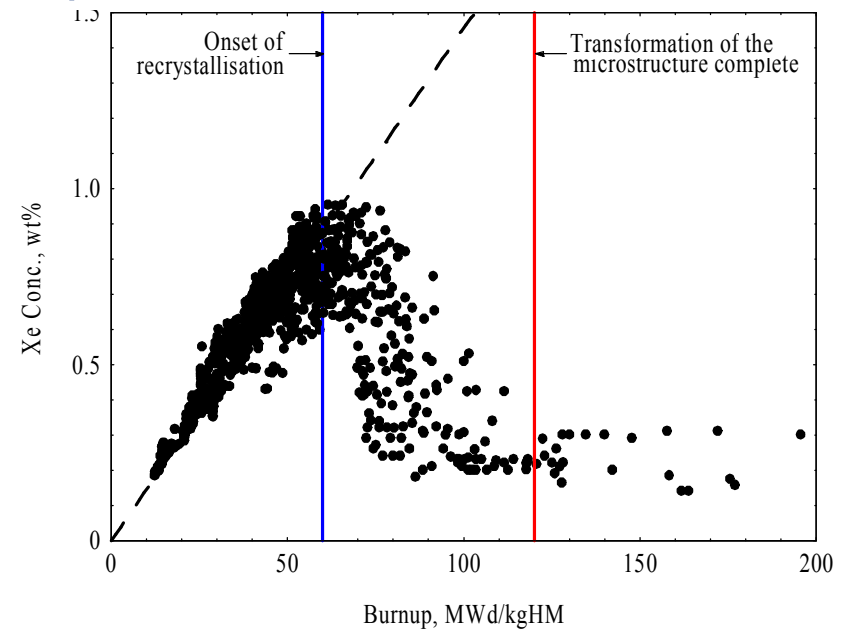


Scanning electron micrographs showing the microstructure in the surface region of  $\text{UO}_2$  fuel at burn-ups below and above a pellet burn-up of 40 MWd/kgU at which recrystallisation of the  $\text{UO}_2$  grains begins. (a) Fuel microstructure at 30 MWd/kgU; (b) fuel microstructure at 45 MWd/kgU.

## EPMA Xe profiles for the estimation of the high burn-up radial extent in a fuel pellet

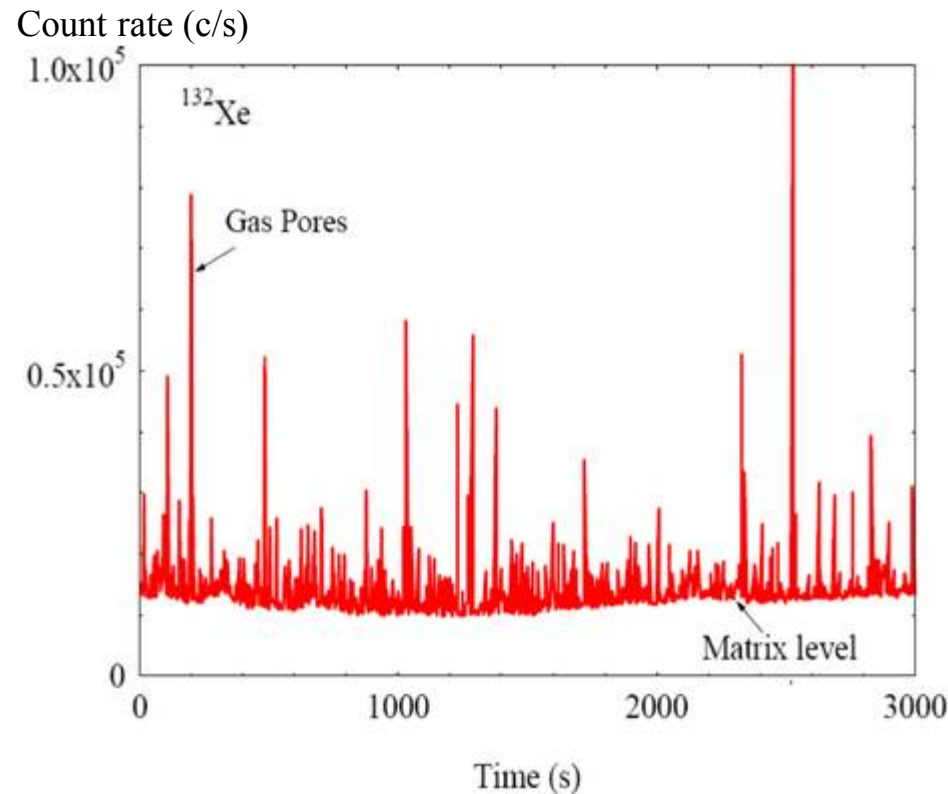


Typical radial distribution profile of Xe in a conventional pressure water reactor fuel.

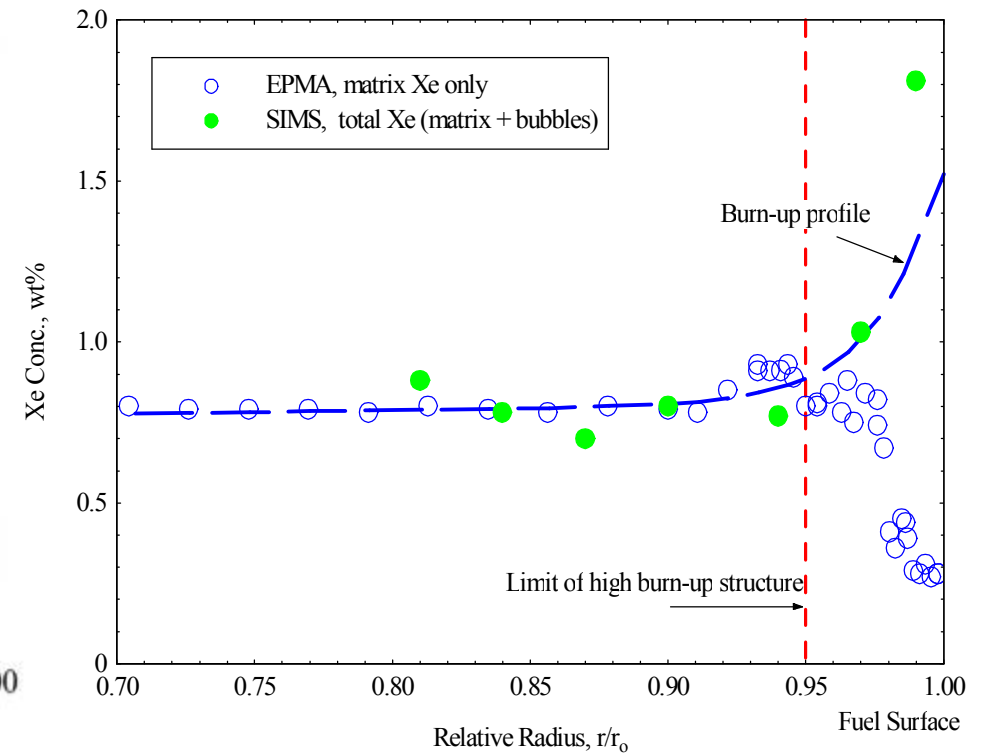


Xe concentration measured in the outer regions of UO<sub>2</sub> fuel as a function of the local burn-up.

## Distribution of the Fission Gas in the HBS

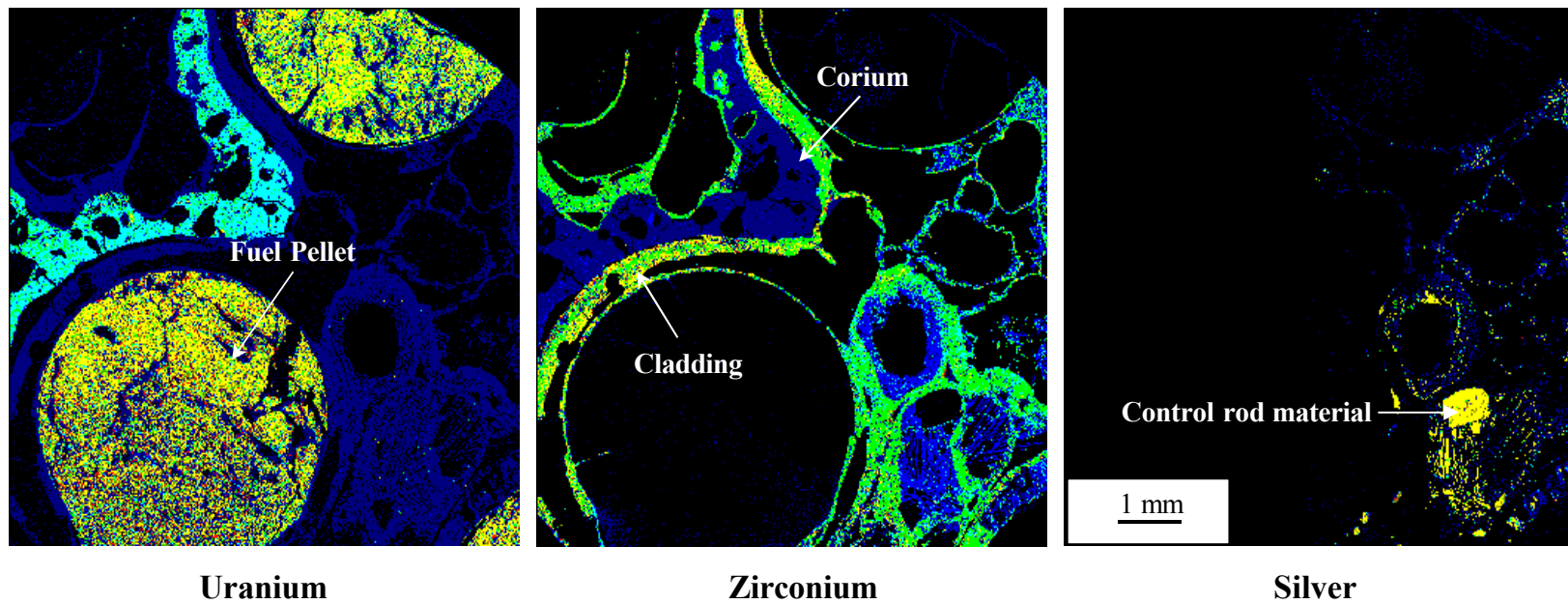


SIMS depth profile for  $^{132}\text{Xe}$  in the high burn-up structure. The intensity spikes are caused by the expulsion of gas from the pores in the microstructure.



The local concentration of retained Xe in the outer region of a high burn-up  $\text{UO}_2$  fuel. The steep increase in the SIMS profile at the fuel surface **indicates that almost all the gas missing from the  $\text{UO}_2$  matrix is contained in the pores of the high burn-up.**

## Degradation of fuel assembly during core melt-down



Fuel rods, Zircaloy cladding (the fuel containment), corium and control rod material in the zone below the corium pool in the melted Phebus FPT2 fuel rod test assembly as revealed by large area, false colour, X-ray maps for U, Zr and Ag.



## Conclusions

- \* There has always been a synergetic relationship between EPMA and the nuclear power industry. Both were born in the 1950s, and in the 1960s EPMA and the civil use of nuclear power developed side by side. This was no coincidence.
- \* The small volume of material analysed and the ease of quantification make EPMA the ideal analytical tool with which to study the chemical behaviour of fission products in nuclear fuel.
- \* Almost all that is presently known about the characteristics of the high burn-up structure of nuclear fuel; the mechanism of its formation and the processes contributing to its evolution, has been acquired from studies employing microbeam analysis techniques.
- \* Today, EPMA and a range of other microbeam analysis techniques are providing fundamental information about the behaviour of nuclear fuel at high burn-up and about the performance of fuels and targets designed for the in-pile incineration or transmutation of plutonium and the minor actinides Np, Am and Cm.
- \* The techniques most commonly used are wave-length dispersive electron probe microanalysis, scanning electron microscopy and secondary ion mass spectrometry. Other microbeam analysis techniques that have been successfully applied to irradiated nuclear fuel are transmission and replica electron microscopy, X-ray fluorescence and micro X-ray diffraction.
- \* In recent years one of the important tasks of EPMA and SIMS at ITU has been the provision of experimental data for the validation of fuel performance codes used by fuel vendors and the operators of nuclear power plants to obtain licences from their national regulatory authority.